Available online at www.sciencedirect.com
SCIENCE DIRECT®
Journal of Power Sources 152 (2005) 189–195
JOURNAL OF POWER SOURCES
www.elsevier.com/locate/jpowsour

Short communication

Test of a water–gas-shift reactor on a 3 kW_e-scale—design points for high- and low-temperature shift reaction☆

J. Pasel*, R.C. Samsun, D. Schmitt, R. Peters, D. Stolten

Forschungszentrum Jülich GmbH, Institute for Materials and Processes in Energy Systems (IWV 3), D-52425 Jülich, Germany

Received 29 November 2004; accepted 24 December 2004
Available online 3 March 2005

Abstract

The amount of carbon monoxide in the reformate from the autothermal reforming of liquid hydrocarbons can be significantly reduced by means of the water–gas-shift reaction. It is possible to directly feed the reformate from the autothermal reforming to the water–gas-shift reactor without deactivation of the catalyst. The results of this paper show a clear advantage of the isothermal operation of a water–gas-shift reactor over the adiabatic mode. Thermodynamic equilibrium was reached at clearly lower temperatures in the case of isothermal operation. A two-stage water–gas-shift reactor with a high-temperature shift part running at a gas hourly space velocity (GHSV) of 42,200 h^{-1} and an inlet temperature of 400 °C and a low-temperature shift stage operated at a GHSV of 26,000 h^{-1} and an inlet temperature in the range between 280 and 310 °C is able to reduce the carbon monoxide outlet concentration to less than 1 vol.%. This reactor will be suitable for combination with a reactor for the preferential oxidation of carbon monoxide in a fuel processing system. The injection of water between the two shift stages is meaningful because carbon monoxide conversion is enhanced by higher partial pressures of water. Furthermore, the injection of water can be applied to cool down the outlet temperature of the high-temperature shift stage of approximately 420 °C to the inlet temperature of the low-temperature shift stage of approximately 300 °C. The latter function can be dispensed with in the case of water injection between autothermal reforming and the high-temperature shift stage, which therefore reduces the positive impact of this step.

Keywords: Autothermal reforming; Water–gas-shift reaction; Hydrogen; Fuel cell

1. Introduction

An important requirement for the polymer electrolyte fuel cell (PEFC) is to have clean hydrogen (H_2) at its anode electrode, the oxidation kinetics of which are strongly decelerated by small amounts of carbon monoxide (CO). Within fuel processing, CO is produced in the upstream autothermal reforming (ATR) of, for example, diesel fuel [1–3]. In [4], the upper limit for the concentration of CO entering the fuel cell anode is given as 50 ppm. Therefore, it is essential to integrate several reaction units into the fuel cell system permitting a conspicuous reduction of the CO concentration in the gas mixture from the ATR. A process step, which helps to fulfil these demands, is the heterogeneously catalysed water–gas-shift (WGS) reaction, which proceeds according to the following equation (1):

$$CO + H_20 \rightarrow CO_2 + H_2; \quad \Delta H^0{}_{298} < 0 \tag{1}$$

In [5], a detailed summary is given of the different catalytic systems to be used for the water–gas-shift reaction. In [6,7], it is stated that a reactor for the WGS reaction in a mobile application should be cost-efficient, lightweight, tolerant of road vibrations and capable of rapid start up. In [8], Krumpelt et al. go more into detail and specify target values. For transportation purposes, small fuel cell systems in the range of 1–100 kW with a WGS reactor must not cost more than US$ 100 kW^{-1} to be economically viable. Furthermore, the US Department of Energy Office of Advanced Automotive Technologies (DOE/OAAT) stipulates that in 2008 these systems must be able to undergo multiple startups and shutdowns,

☆ This paper was presented at the 2004 Fuel Cell Seminar, San Antonio, TX, USA.

* Corresponding author. Tel.: +49 2461 61 5140; fax: +49 2461 61 6695.
E-mail address: j.pasel@fz-juelich.de (J. Pasel).

0378-7753/$ – see front matter © 2005 Elsevier B.V. All rights reserved.
doi:10.1016/j.jpowsour.2004.12.051

achieve maximum power from a cold start (−20 °C) in 1 min, respond to changes in the power demand from 10 to 90% in 1 s and have a power density of 800 Wl^{-1} [9]. To be able to meet these goals with respect to the WGS reactor three different commercial catalyst-coated monoliths were tested concerning their catalytic activity. The results of these experiments are given in [5].

For this paper, the most active catalyst among the tested materials, which was found to be a precious metal catalyst, was chosen and assembled into a newly designed and constructed single-stage reactor. This means that this reactor is not divided into a high- and low-temperature section. This reactor of the first generation was directly combined with an autothermal reformer in the power class of 3 kW_e. Isothermal and adiabatic operation conditions of the reactor were studied. In previous work [5], it was found that if convenient reaction conditions were chosen for the autothermal reforming, only traces of impurities were detected in the water stream from the autothermal reformer. Furthermore, no higher hydrocarbons such as benzene or toluene could be found in the product from autothermal reforming. Both the impurities in the water stream and higher hydrocarbons are thought to poison the catalyst for the water–gas-shift reaction and lead to deactivation. Based on the results of the experiments with the single-stage 3 kW_e reactor additional investigations with the same catalyst were performed on a smaller scale to elucidate exact design points with respect to reaction temperature and gas hourly space velocity (GHSV) for a two-stage water–gas-shift reactor of the second generation with spatially separated sections for the high- and low-temperature shift reaction.

2. Experimental

Two sets of experiments were carried out with direct coupling of the shift reactor to the autothermal reformer for the characterisation of the WGS reactor of the first generation. Each experiment was carried out for two different gas hourly space velocities in the shift reactor. Reaction characteristics were analysed by varying the temperature during each experiment. In the isothermal operation mode, the inlet temperature of the shift reactor and the temperature within the shift reactor were adjusted by oil circulation heating. Nevertheless, slight temperature gradients occurred in the axial direction of the reactor. In the adiabatic mode, the inlet temperature of the shift reactor was adjusted by heating oil circulation and the shift reactor was operated without any cooling. Due to heat losses, the temperature decreased in the axial direction of the reactor after the adiabatic temperature rise had occurred. The autothermal reformer was operated with an oxygen/carbon ratio of $n(O_2)/n(C) = 0.47$ and a steam/carbon ratio of $n(H_2O)/n(C) = 1.9$. Two different amounts of hydrocarbon feeds (800 and 400 g/h) and corresponding amounts of steam and air were utilised to achieve two different space velocity profiles within the shift reactor. A C_{13}–C_{15} alkane mixture was used as the hydrocarbon feed. No extra water was added after the reforming stage. The temperature of the circulating heating oil was varied between 170 and 330 °C using a thermostat. A mass spectrometer (Prima 600 S, VG Gas) was used to analyse the mass concentrations at the exit of the reformer and at the exit of the shift reactor. NiCr–Ni thermocouples were located in the axial direction of the shift reactor to monitor the temperature profile within the reactor. Four rows of precious-metal-coated monoliths, each having a length of 62.5 mm and a diameter of 12 mm, were positioned in 17 columns making up the reactor.

The experiments on a smaller scale concerning design points such as reactor inlet temperature and gas hourly space velocity for a two-stage water–gas-shift reactor were done with a single precious-metal-coated monolith having a diameter of 12 mm and a length 62.5 mm in the case of the high-temperature shift (HTS) stage. The monolith coated with precious metals for the low-temperature shift (LTS) stage had a diameter of 12 mm and a length 125 mm. These investigations were divided into three sections:

Section (i): For these experiments the product stream from the autothermal reforming (reformate), which has a temperature of approximately 180 °C, was heated up to approximately 400 °C using a heating band to simulate reaction conditions of a high-temperature shift stage. The GHSV was varied between 42,200 and 181,000 h^{-1} by diversifying the amount of product stream coming from the autothermal reforming using a valve to split the flow and a mass flow meter to determine the exact amount of flow. No extra water was added after the reforming stage. Table 1 gives the average concentrations of all components in the reformate. The concentrations after the reformer and after the shift catalyst were measured with the mass spectrometer mentioned above. The product flow from ATR was generated as described above.

Table 1
Composition of the reformate fed into the high-temperature shift stage in Section (i)

	Concentration (vol.%)
CO	7.4
H_2O	21.6
H_2	28.8
CO_2	10.4
N_2	30.9

Table 2
Composition of the reformate fed into the high-temperature shift stage in Section (ii)

	Concentration (vol.%)
CO	6.5
H_2O	31.4
H_2	25.1
CO_2	9.0
N_2	27.2

Table 3
Reaction conditions of the low-temperature shift stage in Section (iii)

#	GHSV (h^{-1})	T_{inlet} (°C)	$n(H_2O)/n(C)$	$x(CO)_{in}$ (%)	$x(H_2O)_{in}$ (%)	$x(H_2)_{in}$ (%)	$x(CO_2)_{in}$ (%)	$x(N_2)_{in}$ (%)
1	24200	302	1.28	3.2	20.3	31.8	14.1	29.7
2	26000	301	1.73	3.0	25.7	29.7	13.2	27.7
3	26000	292	1.73	3.0	25.7	29.7	13.2	27.7
4	26000	283	1.73	3.0	25.7	29.7	13.2	27.7
5	26000	310	1.73	3.0	25.7	29.7	13.2	27.7

Section (ii): The investigations in Section (ii) only differ from those in Section (i) by the concentrations of the components in the product flow from ATR. Table 2 summarises the concentrations. The concentration of water was increased by the injection of additional water into the reformate to examine the influence of a higher partial pressure of water on CO conversion.

Section (iii): In this section an HTS stage was combined with a LTS reactor under the reaction conditions from Section (i) (cf. Table 1) at a GHSV of 42,200 h^{-1}. Table 3 gives experimental details of the low-temperature shift stage. The experiments differed from each other with respect to their inlet temperature and their $n(H_2O)/n(C)$ ratios. Consequently, slightly different gas hourly space velocities and gas concentrations arose.

3. Results and discussion

3.1. Isothermal operation mode

In the isothermal operation mode, two experiments were run. In the first one, a hydrocarbon feed of 800 g/h was used in the autothermal reformer resulting in a gas hourly space velocity of 14,800 h^{-1} in the shift reactor. In the second experiment, a hydrocarbon feed of 400 g/h was utilised in order to achieve a gas hourly space velocity in the shift reactor of 7100 h^{-1}.

Conversion as a function of exit temperature of the shift reactor for these experiments is presented in Fig. 1. Comparing the results of the two experiments, it can be seen that the first signs of the reaction were observed at about 220 °C with a GHSV of 14,800 h^{-1}, whereas the first signs of the reaction could be found at about 170 °C during the experiment with a GHSV of 7100 h^{-1}. However, the amount of conversion was very low at both points, so these points can only be taken as references for, e.g., an ignition temperature at which the reaction started. Similarly, a conversion of about 50% was achieved at 300 °C in the first experiment compared to 255 °C in the second experiment. At a GHSV of 14,800 h^{-1}, thermodynamic equilibrium was reached at 310 °C. This corresponds to only a 10 K increase in temperature compared to the measurement at 300 °C with 50% conversion. This shows the sensitivity of this region in terms of catalyst activity. The resulting CO concentration was 2.5% in the dry product. In the second experiment, with half of the gas hourly space velocity, equilibrium was reached at 300 °C. The resulting CO concentration was 1.5% in the dry product. A further increase in temperature resulted in a decrease in conversion due to thermodynamic limitations.

These experiments both lead to two important results. As seen in Fig. 1, the catalyst activity at low temperatures is

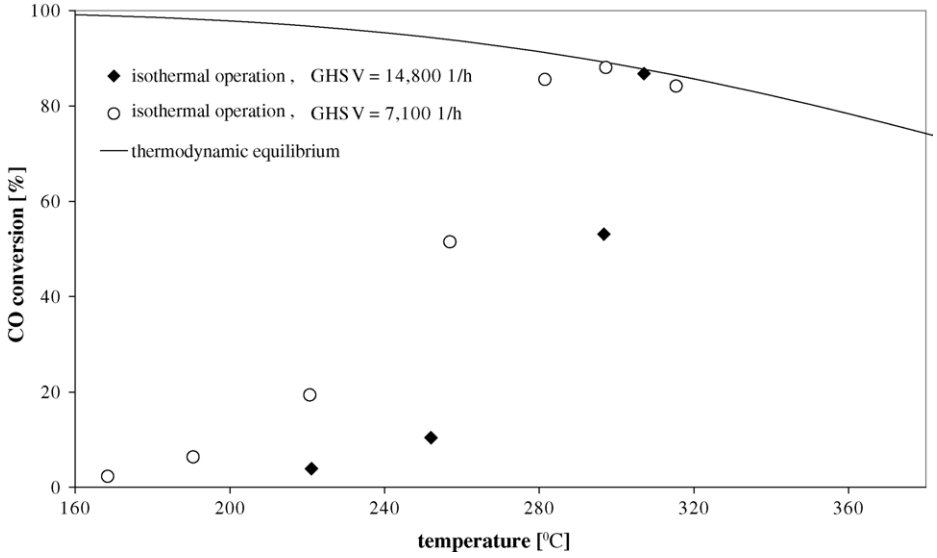

Fig. 1. CO conversion as a function of reaction temperature and gas hourly space velocity with isothermal operation of the reactor for water–gas-shift reaction (reforming: hydrocarbon feed = 800/400 g/h, $n(O_2)/n(C) = 0.47$, $n(H_2O)/n(C) = 1.9$).

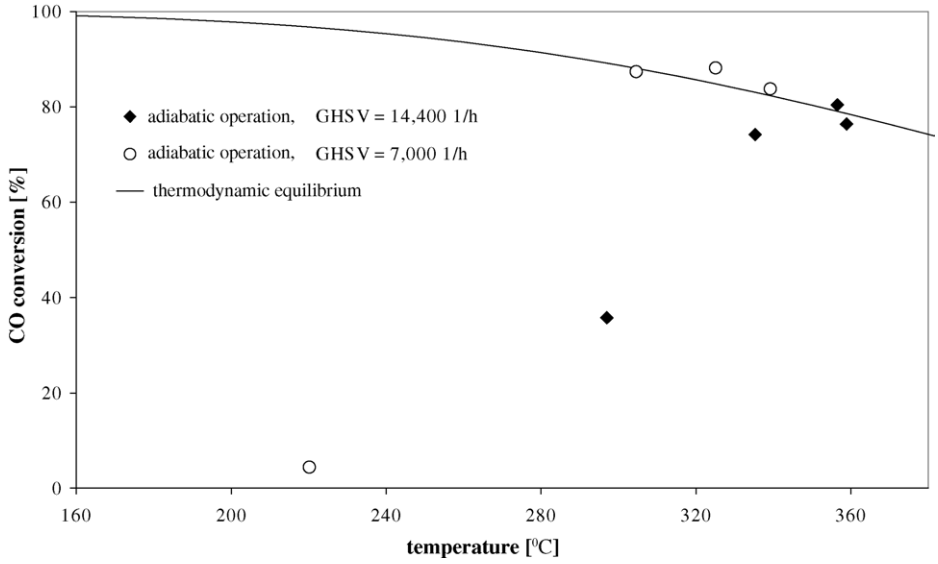

Fig. 2. CO conversion as a function of reaction temperature and gas hourly space velocity with adiabatic operation of the reactor for water–gas-shift reaction, (reforming: hydrocarbon feed = 800/400 g/h, $n(O_2)/n(C) = 0.47$, $n(H_2O)/n(C) = 1.9$).

very poor and is actually limited by reaction kinetics. This eliminates the possibility of reaching high CO conversions at low temperatures with favourable thermodynamics. Secondly, the activity of the catalyst strongly depends on space velocity. The performance in the second experiment with half the space velocity was much better than the first case. This result is obvious, since the educts have twice the residence time in comparison to the first case.

3.2. Adiabatic operation mode

Experiments 3 and 4 represent the experiments without cooling the shift reactor so that adiabatic reaction conditions are achieved. As in the case of experiments in the isothermal operation mode, the difference between experiments 3 and 4 is the changing gas hourly space velocity. In experiment 3, 400 g/h hydrocarbon feed in the autothermal reformer was utilised, resulting in a gas hourly space velocity of 7000 h^{-1} in the shift reactor similar to the second experiment. A hydrocarbon feed of 800 g/h was utilised in experiment 4 resulting in a gas hourly space velocity of 14,400 h^{-1} similar to the first experiment. Fig. 2 presents the conversion in experiments 3 and 4 as a function of the exit temperature of the shift reactor. The experiments for the adiabatic operation mode with two different gas hourly space velocities showed results parallel to the isothermal operation mode. The performance of the catalyst was better with lower load and the start of the reaction was observed at lower temperatures with lower load, as in the previous section. Comparing the experiments of isothermal and adiabatic modes with each other a remarkable difference is observed. Apparently, conversion trends of the second experiment (isothermal operation mode, GHSV = 7100 h^{-1}) and experiment 3 (adiabatic operation mode, GHSV = 7000 h^{-1}) show very similar tendencies. However, observing the two graphs carefully, it can be seen that the trends of the adiabatic case follow the trends of the isothermal case with a difference of about 25 K. The adiabatic system suffers from the high temperatures with respect to thermodynamic constraints. Since thermodynamic equilibrium is reached at higher temperatures, the resulting conversion amounts were lower. Especially in experiment 4 (adiabatic operation mode, GHSV = 14,400 h^{-1}), the thermodynamic equilibrium was reached at about 360 °C where a conversion of only 80% is thermodynamically possible. The temperature difference between the inlet and the middle section of the shift reactor reached 65 K in this experiment.

The results presented above show a clear advantage of the isothermal operation mode over the adiabatic operation mode. Since the results are based on the exit temperature of the shift reactor, the reaction pathways need to be analysed. Ideally, the inlet temperature equals the exit temperature in the isothermal case. To reach the same exit temperature as in the isothermal case, the inlet temperature in the adiabatic case has to be much less than its exit temperature because of the uncontrolled exothermal reaction. Since the reaction kinetics is worse in the case of lower temperatures, the conversion within the first stages of the shift reactor is lower than is the case of the isothermal mode, where the temperatures within the first stages are already as high as the exit temperature. Since the temperature gradient along the axial length (except for the exit temperature) is always lower in the adiabatic mode, the same exit temperatures result in different conversion levels for the different operation modes. In the real case, if the inlet temperature is taken as a reference, the exit temperature in the adiabatic case will be higher than the exit temperature of the isothermal case for two reasons: (i) due to the adiabatic mode of operation the temperature increase inside the monolith is more profound; (ii) in the isothermal

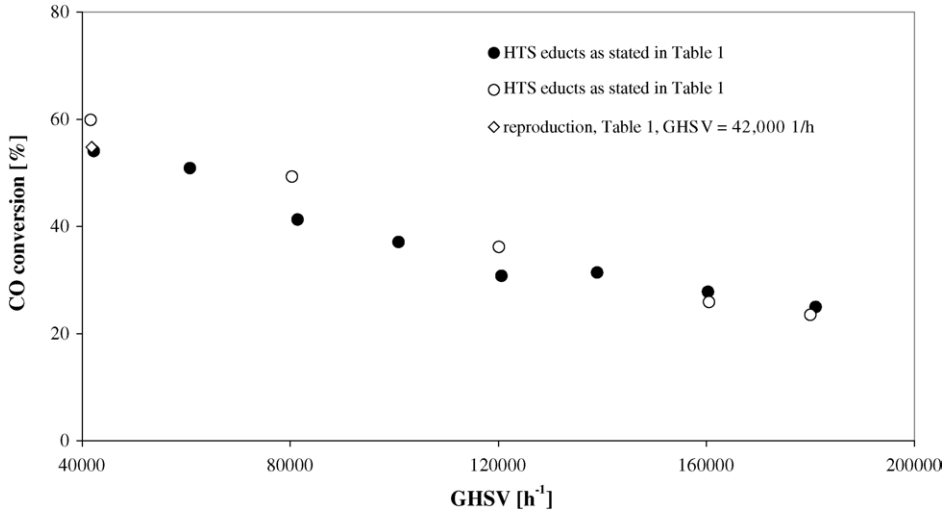

Fig. 3. CO conversion as a function of gas hourly space velocity and two different partial pressures of water in the high-temperature shift stage, l (cat.) = 62.5 mm, d (cat.) = 12 mm, T_{inlet} = 400 °C, concentrations of components as given in Tables 1 and 2.

mode the heating oil provides stronger heat removal resulting in a strong temperature decrease from the middle part of the catalyst to the exit of the shift reactor. Higher exit temperatures will lead to lower CO conversions if the equilibrium is reached. It can be concluded that for both cases isothermal operation mode results in better characteristics. For the adiabatic operation mode, the inlet temperature of the reactor must be selected in such a manner that the exit temperature of the reactor, which is the adiabatic reaction temperature, is too low to reach the thermodynamic equilibrium. In this case, good reaction kinetics is achieved at higher temperatures and the reaction is not limited by equilibrium.

3.3. Design points for reactor inlet temperature and gas hourly space velocity

Section (i) and (ii): Fig. 3 shows CO conversion as a function of gas hourly space velocity at a reactor inlet temperature of 400 °C for two different compositions of the reformate as given in Tables 1 and 2. As expected, CO conversion decreased from 54% at a GHSV of 42,200 h^{-1} to 25% at a GHSV of 181,000 h^{-1} under the reaction conditions of Table 1. Due to lower contact times of the molecules of the reformate with the catalyst fewer of them were able to react with each other according to equation (1). Anyway, it is remarkable in Fig. 3 that a GHSV of approximately 80,000 h^{-1} still allows for a CO conversion of more than 40%, which might be enough for an HTS stage. The experiments with a higher partial pressure of water applying the composition of the reformate given in Table 2 showed that in the range of lower gas hourly space velocities between 42,200 and 120,000 h^{-1} a slight increase in CO conversion could be observed. At a GHSV of approximately 80,000 h^{-1}, the enhancement of CO conversion was most profound from 41% at a water concentration of 21.6 to 49 vol.% at a concentration of water of 31.4%. This result is in good agreement with the findings of Koyabkina et al. [10], who found a reaction order for water of 0.8 on a copper catalyst. A reaction order of 0.8 means that higher partial pressures of water favour the effective reaction rate of the water–gas-shift reaction and lead to higher CO conversions. However, in the range of higher gas hourly space velocities between 160,000 and 180,000 h^{-1} the positive influence of higher concentrations of water could no longer be observed. Obviously, these contact times are too short to yield observable differences with respect to CO conversion. On the one hand, the result that higher concentrations of water in the reformate entering the HTS stage enhance the effective reaction rate of CO removal offer the potential to design and construct water–gas-shift reactors for fuel cell systems with lower weight and volume. However, on the other hand, the complex storage, evaporation and metering of water is an immense problem. This casts doubt upon the injection of additional water between the reformer and HTS stage. Fig. 3 also contains a reproduction experiment under the reaction conditions in Table 1 at a GHSV of 42,000 h^{-1}. The excellent agreement with the previous experiment proves the significance of the statements and conclusions, derived above.

Section (iii): Fig. 4 shows CO conversion as well as the outlet concentration of CO after the LTS stage under the reaction conditions from Table 3. Fig. 4 makes it obvious that an increase in the $n(H_2O)/n(C)$ ratio from experiment 1 to 2 (cf. Table 3), which is equivalent to an increase in the partial pressure of water from 20.3 to 25.7 vol.%, resulted in a slight enhancement of CO conversion. This result confirms the findings from Sections (i) and (ii) concerning the positive effect of higher partial pressures of water on CO conversion. During experiments 2–5 in Fig. 4, the $n(H_2O)/n(C)$-ratio was kept constant at a GHSV of 26,000 h^{-1}, while the inlet temperature of the LTS stage was varied between approximately 280 and 310 °C. No strong dependence of CO conversion on

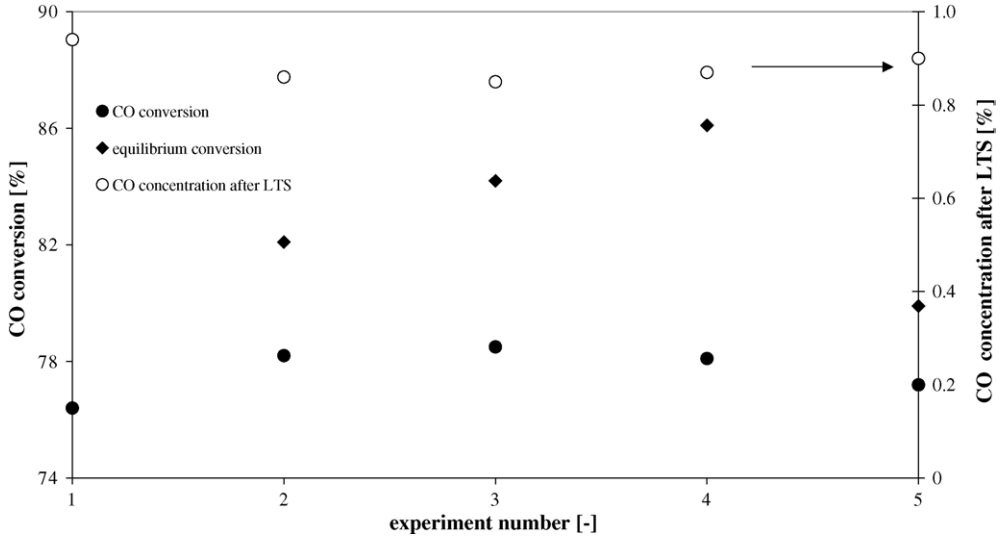

Fig. 4. CO conversion and CO concentration after the low-temperature shift stage, l (cat.) = 125 mm, d (cat.) = 12 mm, further reaction conditions (GHSV; T_{inlet}, concentrations of components) as given in Table 3.

the inlet temperature could be observed. Chemical equilibrium was not reached in any of the experiments.

Fig. 4 shows that the concentration of CO in the product stream of the LTS stage was below 1.0 vol.% (approximately 0.9 vol.%) at each of the five experiments. There are two ways of coming closer to equilibrium and further reducing the concentration of CO after the LTS stage. The first one is to decrease the gas hourly space velocity. Unfortunately, this will lead to a technically irrelevant water–gas-shift reactor, whose volume and weight is too high for an application in a fuel cell system. The second one is to develop new catalysts with higher activity. This has to be done by the catalyst industry.

Nevertheless, the results shown in Fig. 4 mean that a two-stage water–gas-shift reactor with an HTS part running at a GHSV of 42,200 h^{-1} and an inlet temperature of 400 °C and a LTS stage operated at a GHSV of 26,000 h^{-1} and an inlet temperature in the range between 280 and 310 °C is suitable for combination with a reactor for the preferential oxidation of CO. The injection of water between the two shift stages is more meaningful than after the reformer and in front of the HTS stage because in this case it is bifunctional. Firstly, as shown in Figs. 3 and 4, CO conversion is enhanced by higher partial pressures of water and, secondly, the injection of water can be applied to cool down the outlet temperature of the HTS stage of approximately 420 °C to the above-mentioned inlet temperature of the LTS stage of approximately 300 °C. The latter function is essential for the mode of operation of a two-stage water–gas-shift reactor.

4. Conclusions

- The results of this paper presented above show a clear advantage of the isothermal operation mode of a water–gas-shift reactor over the adiabatic way of operation. Thermodynamic equilibrium was reached at clearly lower temperatures in the case of isothermal operation.
- A two-stage water–gas-shift reactor with an HTS part running at a GHSV of 42,200 h^{-1} and an inlet temperature of 400 °C and an LTS stage operated at a GHSV of 26,000 h^{-1} and an inlet temperature in the range between 280 and 310 °C is able to reduce the CO outlet concentration to less than 1 vol.%. This reactor will be suitable for combination with a reactor for the preferential oxidation of CO in a fuel processing system.
- The injection of water between the two shift stages is meaningful because CO conversion is enhanced by higher partial pressures of water and the injection of water can be applied for cooling down the outlet temperature of the HTS stage of approximately 420 °C to the above-mentioned inlet temperature of the LTS stage of approximately 300 °C. The latter function is dispensed with in the case of water injection between ATR and HTS stage and therefore reduces the positive impact of this step.

Acknowledgements

The authors thank Mr. B. Sobotta for valuable technical assistance. The authors are grateful to OMG AG & Co. KG for supplying catalysts for the ATR and for technical discussions.

References

[1] J. Pasel, C. Palm, P. Cremer, R. Peters, D. Stolten, Proceedings of the World Renewable Energy Conference, Cologne, Germany, June 29–July 5, 2002.
[2] C. Palm, P. Cremer, R. Peters, D. Stolten, J. Power Sources 106 (2002) 231.

[3] C. Palm, S. Montel, P. Cremer, R. Peters, D. Stolten, Proceedings of Hypothesis IV, Stralsund, Germany, vol. 1, September 9–14, 2001.
[4] F. Joensen, J.R. Rostrup-Nielsen, J. Power Sources 105 (2002) 195.
[5] J. Pasel, P. Cremer, B. Wegner, R. Peters, D. Stolten, J. Power Sources 126 (2004) 112.
[6] S. Ahmed, M. Krumpelt, Int. J. Hydrogen Energy 26 (2001) 291.
[7] J.R. Rostrup-Nielsen, Phys. Chem. Chem. Phys. 3 (2001) 283.
[8] M. Krumpelt, T.R. Krause, J.D. Carter, J.P. Kopasz, S. Ahmed, Catal. Today 77 (2002) 3.
[9] US Department of Energy, Office of Transportation Technologies, Annual Report, vol. 1, 2001.
[10] N.A. Koryabkina, A.A. Phatak, W.F. Ruettinger, R.J. Farrauto, F.H. Ribeiro, J. Catal. 217 (2003) 233.